35th Annual International Conference of the IEEE EMBS
Osaka, Japan, 3 - 7 July, 2013

On the Least-Square Estimation of Parameters for Statistical Diffusion Weighted Imaging Model

Jing Yuan*, *Senior Member, IEEE*, Qinwei Zhang, *Student Member, IEEE*

***Abstract*— Statistical model for diffusion-weighted imaging (DWI) has been proposed for better tissue characterization by introducing a distribution function for apparent diffusion coefficients (ADC) to account for the restrictions and hindrances to water diffusion in biological tissues. This paper studies the precision and uncertainty in the estimation of parameters for statistical DWI model with Gaussian distribution, i.e. the position of distribution maxima (D_m) and the distribution width (σ), by using non-linear least-square (NLLS) fitting. Numerical simulation shows that precise parameter estimation, particularly for σ, imposes critical requirements on the extremely high signal-to-noise ratio (SNR) of DWI signal when NLLS fitting is used. Unfortunately, such extremely high SNR may be difficult to achieve for the normal setting of clinical DWI scan. For D_m and σ parameter mapping of *in vivo* human brain, multiple local minima are found and result in large uncertainties in the estimation of distribution width σ. The estimation error by using NLLS fitting originates primarily from the insensitivity of DWI signal intensity to distribution width σ, as given in the function form of the Gaussian-type statistical DWI model.**

I. INTRODUCTION

Diffusion-weighted imaging (DWI) is capable of noninvasively measuring water diffusivity in living tissues and is growing rapidly in scope and importance for clinical applications [1, 2]. The displacement of a freely mobile water molecule diffusing from one location to another in a certain time is traditionally considered to be Gaussian distributed. Upon this assumption, DWI signal intensity is normally modeled as a mono-exponential decay with increasing b-value [3] and apparent diffusion coefficient (ADC) can be calculated to quantitatively evaluate the average water diffusivity in tissues. However, due to the complexity of heterogeneous cellular structures in tissues, the motion of water is hindered by many barriers like cell membranes and hence leads to the substantial deviation of DWI signal from the mono-exponential decay [4]. In recently years, many diffusion models different from the mono-exponential model have been proposed to account for the non-Gaussianality of DWI in living tissues, particularly in brain, [5-12]. Statistical DWI model has been proposed by Yablonskiy *et al* [10] to better describe the DWI signal attenuation by introducing a statistical distribution function for ADC. At least two parameters of the distribution function, i.e., the position of distribution maxima (D_m) and the distribution width (σ), can be utilized for better tissue characterization from this statistical model rather than the single ADC in the mono-exponential DWI model. Both D_m and σ have potentials to be used as the biomarkers for diseases, but one important pre-requisite is that their values should be able to be accurately and precisely quantified from the measurement. Linear least-square fitting (LLS) and non-linear least-square fitting (NLLS) are the most widely-applied methods for parameter quantification in MRI studies. In this study, accuracy and uncertainty in the estimation of D_m and σ by using NLLS fitting are investigated by numerical simulation as well as *in vivo* brain DWI mapping. The pitfalls of statistical model parameter estimation by NLLS fitting are discussed and the source of estimation error is analyzed.

*Research supported by Hong Kong GRC grant SEG_CUHK02.

J. Yuan (corresponding author, jyuan@cuhk.edu.hk) and Q. Zhang are with the Department of Imaging and Interventional Radiology, The Chinese University of Hong Kong, Shatin, NT, Hong Kong, China. J. Yuan is also with the CUHK Shenzhen Research Institute, Guangdong, China.

II. METHODS

A. Numerical Simulation

The statistical model for DWI assumes a continuous distribution of diffusion coefficient (*D*) due to the complexities of tissues. As such, DWI signal can be written as:

$$S(b) = S_0 \int_0^\infty P(D) e^{-bD} dD \quad (1)$$

where S(b) and S_0 denote the signal intensity obtained with the diffusion gradient b-value of b and zero, respectively. *P(D)* is the distribution function of diffusion coefficient *D*. If *P(D)* is Gaussian distributed, then the analytical form of the statistical model can be written as:

$$S(b) = S_0 \cdot \frac{1 + \Phi\left(\frac{D_m}{\sigma\sqrt{2}} - \frac{b\sigma}{\sqrt{2}}\right)}{1 + \Phi\left(\frac{D_m}{\sigma\sqrt{2}}\right)} e^{-(b \cdot D_m + \frac{1}{2} b^2 \sigma^2)} \quad (2)$$

where D_m and σ are the position of maxima and the width of the Gaussian distribution for diffusion coefficient.

Estimation of D_m and σ by NLLS fitting was performed by Monte Carlo simulation implemented in MATLAB (MathWorks, Natick, MA, USA). DWI signal was generated according to Eq. (1) using different pre-assigned D_m and σ values. Rician noise was imposed on ideal DWI signal and its average level was determined by the assigned signal-to-noise ratio (SNR) relative to S_0. Note that Rician noise approaches Gaussian noise if SNR is moderately high, e.g. SNR>10. To avoid the zero or negative diffusivities, σ values were restricted by $\sigma<0.4\ D_m$. b-factors were set as 0-5 ms/μm^2 with an increment of 0.25 ms/μm^2. Noise imposed DWI signal was then NLLS fitted to Eq. (2) based on Levenberg-Marquardt

algorithm. The fitted values of D_m and σ were restricted to be larger than zero. This procedure repeated 50,000 times for each set of true D_m and σ. The statistics of fitting results of D_{mfit} and σ_{fit} were compared to the true values of D_m and σ.

B. *DWI scan and analysis*

MRI scan was performed on a mineral oil phantom and two healthy volunteers at 3T (Philips Healthcare, Best, The Netherlands) using an 8-channel head coil for acquisition. Appropriate ethical approval was obtained. A fat-suppressed single-shot spin-echo EPI (SS-SE-EPI) sequence with a pair of rectangular diffusion gradient pulses along all three orthogonal axes was used for DWI acquisition. Imaging parameters for phantom scan were: TR/TE = 3000ms/55 ms, flip angle (FA) = 90º, number of signal average (NSA) = 32, FOV = 220x220mm, matrix=112x112, slice thickness = 8mm, b-factors: 0-2.5 ms/μm^2 with the increment of 0.25 ms/μm^2. Imaging parameters for human brain DWI were: TR/TE = 3000ms/55ms, FA=90º, NSA=32, FOV=230x230mm, matrix=136x108, slice number/thickness = 3/4mm, b-factors: 0-2.5 ms/μm^2 with the increment of 0.25 ms/μm^2.

DWI images were registered first to the baseline image with b=0 to compensate for any possible motion and then exported to a workstation computer for further analysis. Pixel-by-pixel maps of D_m and σ were computed by using NLLS fitting based on Levenberg-Marquardt algorithm with different setting of upper limits for σ fitting.

III. RESULTS

A. *Numerical simulation*

The fitting results of parameter estimation for statistical and mono-exponential diffusion model by NLLS fitting in Monte Carlo simulation are illustrated in Fig. 1.

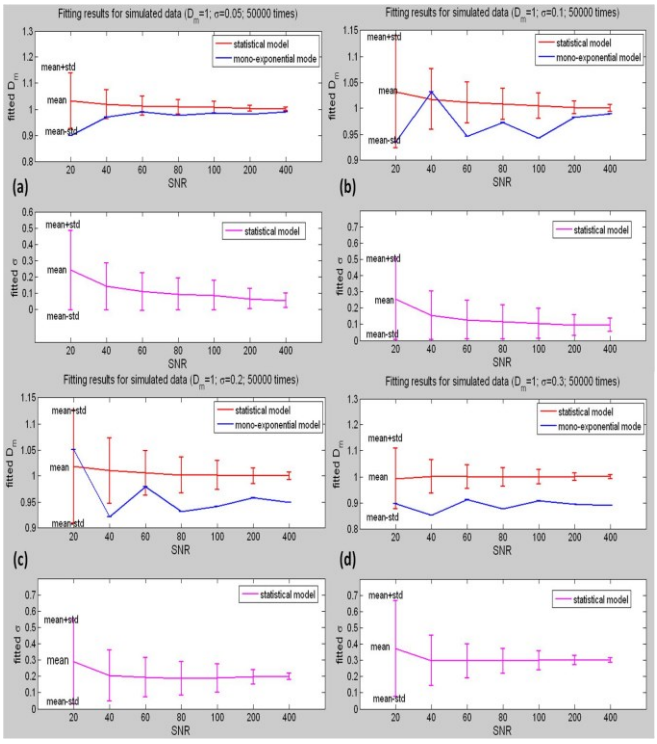

Fig. 1. Non-linear least-square fitting results of parameters in statistical and mono-exponential diffusion model by Monte Carlo simulation. True values for simulation: (a) D_m=1.0, σ=0.05; (b) D_m=1.0, σ=0.10; (c) D_m=1.0, σ=0.20; (d) D_m=1.0, σ=0.30. The units for D_m and σ are both μm^2/ms.

At the very small σ value like 0.05 μm^2/ms, the statistical diffusion was very close to the mono-exponential decay. Consequently, the true value of diffusion coefficient could be accurately estimated by both diffusion models as seen by the mean diffusivity fitting results in Fig. 1a. With the increase of σ, the DWI signal deviated considerably from the mono-exponential decay, so the statistical DWI model supposed to better characterize the DWI signal behavior by providing additional parameters for diffusion description. The fitting accuracy and uncertainty for both D_m and σ were dependent on SNR. In general, fitting accuracy increased while fitting uncertainty decreased with SNR. However, the precision of σ fitting were much worse than D_m fitting, particularly for low σ values at low SNRs. For example, even at the low SNR of 20, the fitted mean D_m were all close to the true value of 1 μm^2/ms and the standard deviations (STD) were generally smaller than 10% of the true D_m. As comparison, the fitted mean σ severely deviated from the true value at low SNRs, and the standard deviations were generally larger than 100% of the true σ, up to around 500% for true σ of 0.05 μm^2/ms at the SNR of 20 (Fig. 1a). Accurate estimation of σ by using NLLS fitting imposed critical requirement on the high SNR for DWI data acquisition. As seen in Fig. 1, only at very high SNR>200, σ could be accurately estimated if the true σ was larger than 0.1 μm^2/ms.

B. *DWI scan*

The NLLS mapping results of D_m and σ for mineral oil phantom DWI scan are shown in Fig. 2.

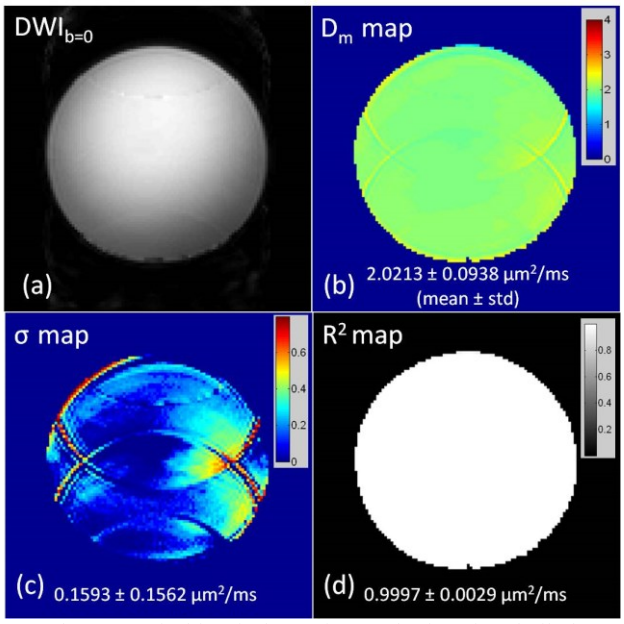

Fig. 2. The NLLS pixel-by-pixel mapping results for mineral oil phantom DWI scan. (a) DWI image acquired at b=0; (b) D_m map; (c) σ map; (d) coefficient of determination (R^2) map.

The diffusion in this mineral oil phantom was considered free, so homogenous diffusivity D_m and a very small

distribution width of diffusivity σ were expected. Excellent goodness of fit were achieved when fitting the DWI signal to the statistical model by NLLS, indicated by the map of coefficient of determination (R^2) (very close to one) as shown in Fig. 2d. The mapping results of D_m were consistent with the expectation very well. A very homogenous D_m of 2.02 was obtained with a small standard deviation of 0.09 $\mu m^2/ms$ even including the slightly higher diffusivities at the ghost artifacts for EPI sequence and the phantom edges. However, in sharp contrast, even with the excellent goodness-of-fit, the variability in the mapping of σ was quite large, ranging from around 0 to 0.8 $\mu m^2/ms$, as shown by the histogram of σ mapping results in Fig. 3. This result was in contradiction to the underlying truth of a homogenous small σ in free diffusion.

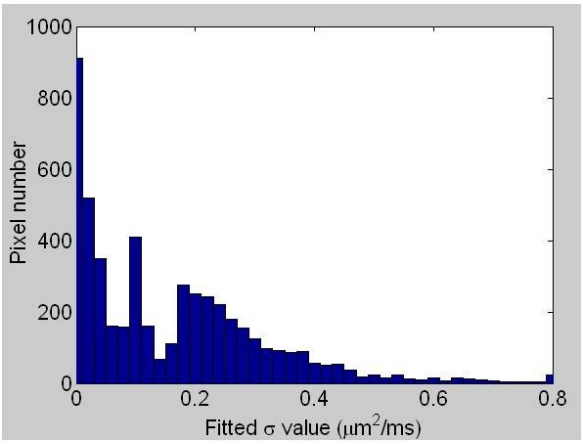

Fig. 3. The histogram of NLLS pixel-by-pixel mapping results of σ. Although the diffusion of mineral oil is considered free and should have very narrow diffusion distribution width σ. The NLLS fitting results show σ values range widely from almost zero to 0.8 $\mu m^2/ms$, but with excellent goodness of fit (R^2 close to one).

For human brain DWI, the maps of D_m and σ by using different upper limits of σ are shown in Fig. 4. As seen in Fig. 4, contradicted to the heterogeneous anatomies of brain, very homogeneous σ values were obtained through NLLS fitting in almost the entire brain, including gray matter, white matter and cerebral spinal fluid (CSF). Within a very wide fitting range for σ, most pixels were almost least-square fitted to the upper limits of σ values, with very high R^2 close to one and without significant difference in D_m fitting results. In other words, there were more than one set of D_m and σ, each of which yielded a minimum in the sum of the squares of the residuals with a very small difference to each other.

IV. Discussion

In this study, precision and uncertainty of the estimation of D_m and σ for statistical DWI model based on Gaussian distribution function by using NLLS fitting were investigated by Monte Carlo simulation as well as phantom and in vivo brain DWI examination. The results showed that the true value of D_m could be accurately and reliably estimated, even at relatively low SNRs. In sharp contrast, the estimation of σ could be significantly deviated from the true value along with large uncertainties, particularly for the small true values of σ at low SNRs. At extremely high SNRs, the precision in the estimation of σ could be much improved. Unfortunately, these high SNRs, however, could be difficult to achieve under normal DWI scan settings.

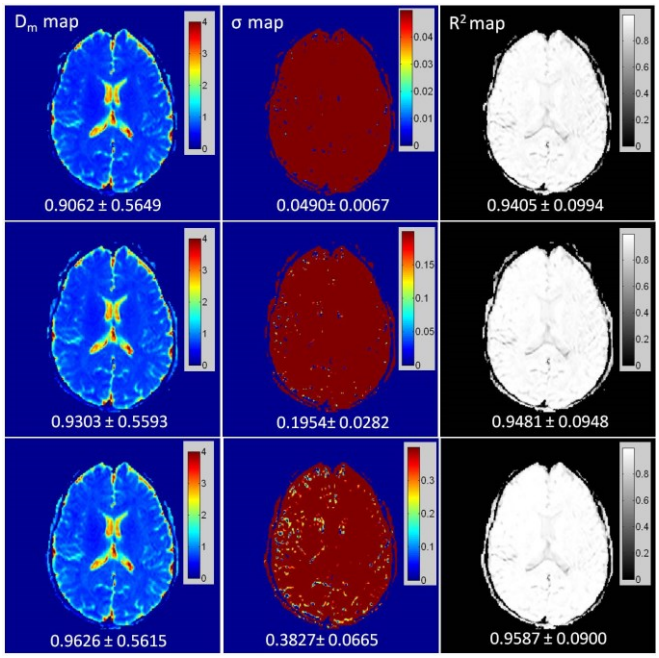

Fig. 4. The NLLS mapping results for human brain DWI scan. The three columns from left to right correspond to the D_m map, σ map and coefficient of determination (R^2) map, respectively. The three rows from top to bottom correspond to the mapping results by setting the upper limits of σ fitting to 0.05 $\mu m^2/ms$, 0.20 $\mu m^2/ms$ and 0.40 $\mu m^2/ms$, respectively. The lower limits and start points for both D_m and σ were set as 1e-4 $\mu m^2/ms$. The upper limit for D_m was set as a sufficiently high value of 10 $\mu m^2/ms$. Multiple local minima for σ were obtained without significant differences in D_m and R^2.

The mapping results of D_m and σ in phantom and human brain DWI agreed with the numerical simulation results well. For phantom DWI, the SNRs of DWI images were intentionally enhanced by large pixel size, very thick slice and large NSA. The diffusion of mineral oil was considered free and homogeneous, which was also verified by the homogenous and high D_m values of about 2.0 $\mu m^2/ms$, so its distribution width of diffusivity supposed to be narrow, approaching to delta function. However, the variability of the estimated σ was quite large (from 0 to 0.8 $\mu m^2/ms$), contradicting to the underlying physical truth. On the other hand, the anatomy of brain and hence its diffusivity supposed to be heterogeneous. Whereas, quite uniform σ was estimated through NLLS fitting for different tissues of white matter, gray matter and CSF. In addition, multiple local minima for σ fitting were observed within a wide range without compromising the goodness of fit much, imposing difficulties in the accurate and reliable quantification of the true σ.

The inaccuracy and uncertainty in the estimation of σ might be attributed to either the pitfalls in NLLS fitting or the intrinsic properties of the statistical diffusion model itself.

According to the R^2 closed to one obtained in both simulation and experiment, the DWI data were all well fitted to the statistical model. Thus, it is unlikely that the algorithms

of NLLS account primarily for the inaccuracy and uncertainty of σ. In addition, the true value range of σ is difficult to be located through the improvement in the setting for NLLS fitting without reliable prior knowledge of true σ. Numerically, once NLLS converges to a minimum, there might be no guaranteed means of determining whether it is a unique or even the global minimum. Furthermore, even the global minimum might be located by assigning a wide range of σ for NLLS fitting, but this global minimum might show only trivial improvement in terms of R^2 or root mean squared error compared to other local minima. More importantly, as we found in our brain DWI mapping, the global minimum tended to yield best-fitted values of D_m around zero and very large $\sigma >> D_m$ if no fitting restrictions were imposed, resulting in the diffusivity distribution at zero and negative values, which was inconsistent with the underlying physics.

After excluding the pitfalls in NLLS fitting, we have to analyze the numerical properties of the function form of Eq. (2) for the statistical DWI model to trace the source of errors in the estimation of σ. The full analysis of numerical stability for Eq. (2) requires the partial derivatives of DWI signal to σ at different D_m and b values, and the analytical expression of these partial derivatives could be complicated. Here a simple example is illustrated to show the low sensitivity of DWI signal to the variation of σ, as shown in Fig. 5.

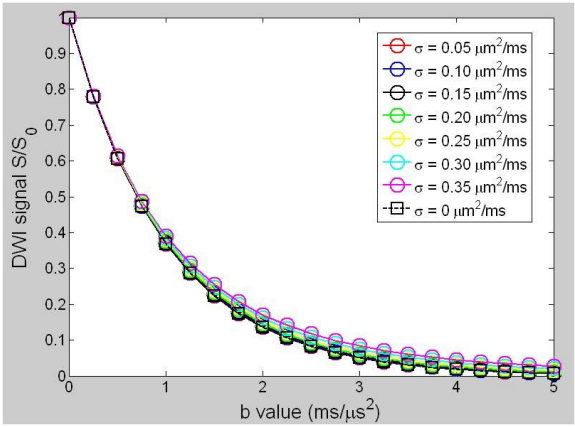

Fig. 5. The low sensitivity of DWI signal to the variation of σ. With a fixed D_m of 1.0 μm^2/ms, the increase of σ from 0 to 0.35 μm^2/ms induces very small change in DWI signal intensity.

In Fig. 5, theoretical DWI signal decay curves without any noise are plotted with a fixed D_m of 1.0 μm^2/ms and varying σ from 0 to 0.35 μm^2/ms. The DWI curves with $\sigma <= 0.25$ μm^2/ms are almost undistinguishable due to the small differences between them, in particular for DWI intensities at low b values. Although the intensity difference becomes noticeable when σ is larger than 0.3 μm^2/ms, these small differences could be easily confounded by the noise contamination. Although Fig. 5 is only valid for D_m of 1.0μm^2/ms, the insensitivity of DWI signal to σ could be easily extended to a wide range of D_m.

Because of this insensitivity of DWI signal to σ, the estimation of σ by using NLLS or other fitting could lead to large deviations from the true values along with large uncertainties. To accurately estimate σ, extremely high SNR is required, but such a high SNR may be difficult to achieve in the normal setting of DWI scan in clinical practice. In addition, this requirement on high SNR is regardless of the statistical profile of noise distribution, although only Rician noise was involved in simulation and non-central Chi distribution was involved in multi-coil acquisition. Note that the insensitivity of DWI signal to σ is only valid for the assumption of Gaussian distribution of diffusivities associated with Eq. (2). For other statistical distribution like gamma function, it is yet to be further studied individually.

V. Conclusion

In principle, statistical diffusion model based on Gaussian distribution function could better describe DWI signal in living tissues by providing more physically meaningful parameters than the mono-exponential model. By using NLLS fitting, D_m can usually be accurately estimated. However, large estimation errors and uncertainties of σ can be produced through NLLS fitting even with the optimization in DWI imaging protocols to enhance SNR. These errors and uncertainties are attributed to the insensitivity of DWI signal intensity to σ as given in its analytical form.

References

[1] D. M. Koh and D. J. Collins, "Diffusion-weighted MRI in the body: applications and challenges in oncology," *AJR Am J Roentgenol,* vol. 188, pp. 1622-35, Jun 2007.

[2] G. P. Winston, "The physical and biological basis of quantitative parameters derived from diffusion MRI," *Quant Imaging Med Surg,* vol. 2, pp. 254-65, Dec 2012.

[3] E. O. Stejskal and J. E. Tanner, "Spin Diffusion Measurements: Spin Echoes in the Presence of a Time-Dependent Field Gradient," *Journal of Chemical Physics,* vol. 42, pp. 288-292, 1965.

[4] D. Le Bihan, "The 'wet mind': water and functional neuroimaging," *Phys Med Biol,* vol. 52, pp. R57-90, Apr 7 2007.

[5] D. Le Bihan, "Intravoxel incoherent motion imaging using steady-state free precession," *Magn Reson Med,* vol. 7, pp. 346-51, Jul 1988.

[6] D. Le Bihan, E. Breton, D. Lallemand, M. L. Aubin, J. Vignaud, and M. Laval-Jeantet, "Separation of diffusion and perfusion in intravoxel incoherent motion MR imaging," *Radiology,* vol. 168, pp. 497-505, Aug 1988.

[7] X. J. Zhou, Q. Gao, O. Abdullah, and R. L. Magin, "Studies of anomalous diffusion in the human brain using fractional order calculus," *Magn Reson Med,* vol. 63, pp. 562-9, Mar 2010.

[8] M. G. Hall and T. R. Barrick, "From diffusion-weighted MRI to anomalous diffusion imaging," *Magn Reson Med,* vol. 59, pp. 447-55, Mar 2008.

[9] J. H. Jensen, J. A. Helpern, A. Ramani, H. Lu, and K. Kaczynski, "Diffusional kurtosis imaging: the quantification of non-gaussian water diffusion by means of magnetic resonance imaging," *Magn Reson Med,* vol. 53, pp. 1432-40, Jun 2005.

[10] D. A. Yablonskiy, G. L. Bretthorst, and J. J. Ackerman, "Statistical model for diffusion attenuated MR signal," *Magn Reson Med,* vol. 50, pp. 664-9, Oct 2003.

[11] K. M. Bennett, K. M. Schmainda, R. T. Bennett, D. B. Rowe, H. Lu, and J. S. Hyde, "Characterization of continuously distributed cortical water diffusion rates with a stretched-exponential model," *Magn Reson Med,* vol. 50, pp. 727-34, Oct 2003.

[12] D. A. Yablonskiy and A. L. Sukstanskii, "Theoretical models of the diffusion weighted MR signal," *NMR Biomed,* vol. 23, pp. 661-81, Aug 2010.